# A Simulation Model and $H_\infty$ Loop shaping Control of a Quad Rotor Unmanned Air Vehicle

Ming Chen * Mihai Huzmezan †
Department of Electrical and Computer Engineering,
University of British Columbia,
Vancouver, BC, Canada, V6T 1Z4

## Abstract

Unmanned Air Vehicles (UAVs) have generated considerable interest in the control and commercial community due to advantages over manned systems for several decades. In this work we are concentrating on the nonlinear modelling of the quad rotor UAV. A flying mill is also presented for flight testing. Linearized models obtained in a quasi-LPV or Jacobian fashion can be used as a starting point for robust control design via Hinf loop shaping. Based on this nonlinear model, a $H_\infty$ loop shaping flight controller is designed for position control.

**Keywords:** Nonlinear Modelling, Quad Rotor UAV, flying mill, $H_\infty$ Loop Shaping Control.

## 1. Introduction

UAVs, or 'Unmanned Air Vehicles,' are defined as aircrafts without the onboard presence of pilots [6]. UAVs have been used to perform intelligence, surveillance, and reconnaissance missions. The technological promise of UAVs is to serve across the full range of missions, including areas such as communications relay and Suppression-of-Enemy-Air-Defenses (SEAD) missions. Cutting edge techniques in sensors, actuators, communications modelling and robust control can make commercial and military missions involving UAVs a reality.

UAVs have several basic advantages over manned systems including increased maneuverability, reduced cost, reduced radar signatures, longer endurance, and less risk to crews. Vertical take-off and landing type UAVs exhibit even further advantages in the maneuverability features. Such vehicles are to require little human intervention from take-off to landing.

Affordability is the key word when building and controlling a UAV. A commercial UAV Draganflyer III quad rotor helicopter was considered by our team as a starting point for more complex missions involving cooperative control and formation flying. This instrument vehicle has significant autonomy required for civilian and military observation missions in a full scale version.

The $H_\infty$ loop shaping flight controller design procedure combines classic loop shaping and notion of bandwidth with model $H_\infty$ robust stabilization. This method which was first proposed by McFarlane and Glover [4] has now been widely used. Significant attempts were made in the aerospace industry. In 1994 [8], $H_\infty$ loop shaping controller was used for position control for a radio controlled helicopter at hover. In 1996 [7], a fixed gain two-degree-of-freedom $H_\infty$ loop shaping controller was designed for the Westland Lynx multirole combat helicopter. The two-degree-of-freedom architecture is more insensitive to disturbance and model uncertainty. In 1999 [5], a new linear parameter-varying (LPV) $H_\infty$ loop shaping design procedure was proposed to design a flight controller for the pitch dynamics of the VAAC Harrier. In this approach the nonlinear model of the VAAC Harrier is approximated by a "quasi-LPV" model. The control law is then automatically scheduled over the flight envelope using this quasi-LPV model. In 2001 [2], the two degree of freedom control architecture and recent advances in parameter-space control design techniques (Odenthal and Blue, 2000) were combined to form a new approach for designing flight controllers for high performance aircraft throughout a large design envelope. This technique extends traditional parameter-space methods to enable the mapping of frequency response specifications into the parameter-space providing a straightforward way of selecting the gains in a fixed control structure to satisfy $H_\infty$ robustness and performance specifications.

In this paper, we first present the nonlinear four-rotor helicopter model and its corresponding SIMULINK model. Next, a reliable testing flying mill is addressed. To achieve the UAV autopilot, $H_\infty$ loop shaping flight controller defined in an initial non-scheduled form is implemented to fulfill the control objectives based on the nonlinear position control model.

## 2. Nonlinear Four-rotor Helicopter Model

The UAV used in the project is a commercial four-rotor helicopter, Draganflyer III, currently with a 3 min flying time but extensible to 1 hour by adequate sizing of the power source and actuators. Four-rotor helicopters using the variant rotor speeds to change the lift forces are dynamically unstable and therefore a control law is permanently required to ensure their stability. Motions of the four-rotor helicopter can be briefly described in Figure 1.

*e-mail: mingc@ece.ubc.ca
†e-mail: huzmezan@ece.ubc.ca

| Symbol | Definition |
|---|---|
| $u(1)$ | $u(1) = F_1 + F_2 + F_3 + F_4$ |
| $u(2)$ | $u(2) = F_4 - F_2$ |
| $u(3)$ | $u(3) = F_3 - F_1$ |
| $u(4)$ | $u(4) = F_1 - F_2 + F_3 - F_4$ |
| $F_{xB}$,$F_{yB}$,$F_{zB}$ | force in body-axis x,y,z direction |
| $F_x$,$F_y$,$F_z$ | force in earth-axis x,y,z direction |
| $I_x$,$I_y$,$I_z$ | moment of inertia in x,y,z direction |
| $p$,$q$,$r$ | roll rate,pitch rate,yaw rate |
| $\phi$,$\theta$,$\psi$ | roll angle,pitch angle,yaw angle |
| $u_B$,$v_B$,$w_B$ | velocity in body-axis x,y,z direction |
| $u$,$v$,$w$ | velocity in earth-axis x,y,z direction |
| x,y,z | COG in earth-axis x,y,z direction |

Table 1: The nomenclature used in theoretical formulation

The vertical motions along z-axis in the body-fixed frame can be obtained by changing the speeds of all the four rotors simultaneously. The forward motions along x-axis in the body-fixed frame can be achieved by changing the speeds of rotor 1 and 3 reversely and retaining the speeds of rotor 2 and 4. The lateral motions along y-axis in the body-fixed frame can be reached by changing the speeds of rotor 2 and 4 reversely and retaining the speeds of rotor 1 and 3. The yaw motions are related to the difference between the moments created by the rotors. To turn in a clock-wise direction, rotor 2 and 4 should increase speeds to overcome the speeds of rotor 1 and 3. The x,y axis definition becomes arbitrarily since the structure presents x,y symmetry.

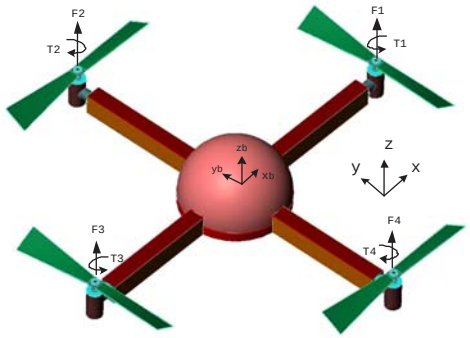


Figure 1: The Four-rotor Helicopter Model

Table 1 summarizes the nomenclature used in the theoretical formulation and further in the SIMULINK model of the four-rotor helicopter, Draganflyer III. This nomenclature is based on GARTEUR notations [1].

The rotational transformation matrix between the earth-fixed frame and the body-fixed frame can be obtained based on Euler angles:

$$R_{EB} = R_\psi \cdot R_\theta \cdot R_\phi =$$

$$\begin{bmatrix} c\psi c\theta & -s\psi c\phi + c\psi s\theta s\phi & s\psi s\phi + c\psi s\theta c\phi \\ s\psi c\theta & c\psi c\phi + s\psi s\theta s\phi & -c\psi s\phi + s\psi s\theta c\phi \\ -s\theta & c\theta s\phi & c\phi c\theta \end{bmatrix}$$

Note that $R_{EB} = R_{BE}^T$ and $s$ and $c$ represent $sin$ and $cos$, respectively.

The transformation of velocities between body-fixed and earth-fixed coordinates is then:

$$\begin{bmatrix} u \\ v \\ w \end{bmatrix} = R_{EB} \begin{bmatrix} u_B \\ v_B \\ w_B \end{bmatrix} \quad (1)$$

Similarly, the accelerations, rotational velocities, positions, forces and moments can be transformed based on $R_{EB}$ between the coordinate systems.

In the body-fixed frame, the forces are defined as follows:

$$F_B = \begin{bmatrix} F_{xB} \\ F_{yB} \\ F_{zB} \end{bmatrix} = \begin{bmatrix} 0 \\ 0 \\ \sum_{i=1}^{4} F_i \end{bmatrix}$$

In the earth-fixed frame, the forces can be described as:

$$\begin{bmatrix} F_x \\ F_y \\ F_z \end{bmatrix} = R_{EB} \cdot F_B =$$

$$(\sum_{i=1}^{4} F_i) \begin{bmatrix} \sin\psi \sin\phi + \cos\psi \sin\theta \cos\phi \\ -\cos\psi \sin\phi + \sin\psi \sin\theta \cos\phi \\ \cos\phi \cos\theta \end{bmatrix}$$

Therefore, the equations of motion x,y,z in the earth-fixed frame are represented as follows .

$$m \begin{bmatrix} \ddot{x} \\ \ddot{y} \\ \ddot{z} \end{bmatrix} = \begin{bmatrix} F_x - K_1 \cdot \dot{x} \\ F_y - K_2 \cdot \dot{y} \\ F_z - mg - K_3 \cdot \dot{z} \end{bmatrix}$$

where $K_i$ are the drag coefficients. Note that these coefficients are negligible at low speeds. As result the equations of motion can be defined below using force and moment balance.

$$m \begin{bmatrix} \ddot{x} \\ \ddot{y} \\ \ddot{z} \end{bmatrix} = \begin{bmatrix} F_x - K_1 \cdot \dot{x} \\ F_y - K_2 \cdot \dot{y} \\ F_z - mg - K_3 \cdot \dot{z} \end{bmatrix}$$

$$\ddot{\phi} = l(F_3 - F_1 - K_4\dot{\phi})/I_x$$

$$\ddot{\theta} = l(F_4 - F_2 - K_5\dot{\theta})/I_y$$

$$\ddot{\psi} = (M_1 - M_2 + M_3 - M_4 - K_6\dot{\psi})/I_z =$$

$$(F_1 - F_2 + F3 - F4 - K_6^{'}\dot{\psi})/I_z^{'}$$

where $l$ is the length from the center of gravity of the helicopter to each rotor and $M_i$'s are the moments of rotor $i$. $I$ represents the moment of inertia with respect to the

axes and $I_z^{'}$ includes the moment of inertia of z axis and the force to moment scaling factor.

For convenience and compatibility with the control panel of the Futaba radio transmitter used with Draganflyer III, we define the inputs to be:

$$u(1) = F_1 + F_2 + F_3 + F_4$$

$$u(2) = F_4 - F_2$$

$$u(3) = F_3 - F_1$$

$$u(4) = F_1 - F_2 + F_3 - F_4$$

Therefore, the motion equations of motion become:

$$\ddot{x} = \frac{u(1)(\sin\psi\sin\phi + \cos\psi\sin\theta\cos\phi) - K_1 \cdot \dot{x}}{m} \quad (2)$$

$$\ddot{y} = \frac{u(1)(\sin\psi\sin\theta\cos\phi - \cos\psi\sin\phi) - K_2 \cdot \dot{y}}{m}$$

$$\ddot{z} = \frac{u(1)\cos\phi\cos\theta - K_3 \cdot \dot{z}}{m} - g$$

$$\ddot{\theta} = (u(2) - K_5\dot{\theta})l/I_y$$

$$\ddot{\phi} = (u(3) - K_4\dot{\phi})l/I_x$$

$$\ddot{\psi} = (u(4) - K_6^{'}\dot{\psi})/I_z^{'}$$

A quasi-LPV formulation for the above motion equations leads to following LPV model:

$$\frac{d}{dt}\begin{bmatrix}\begin{bmatrix}\dot{x}\\ \dot{y}\\ \dot{z}\\ \dot{\theta}\\ \dot{\phi}\\ \dot{\psi}\\ g\end{bmatrix}\\ \begin{bmatrix}\theta\\ \phi\\ \psi\end{bmatrix}\end{bmatrix} = \begin{bmatrix}0&0&0&0&0&0&0&0&0&0\\ 0&0&0&0&0&0&0&0&0&0\\ 0&0&0&0&0&0&-1&0&0&0\\ 0&0&0&0&0&0&0&0&0&0\\ 0&0&0&0&0&0&0&0&0&0\\ 0&0&0&0&0&0&0&0&0&0\\ 0&0&0&0&0&0&0&0&0&0\\ 0&0&0&1&0&0&0&0&0&0\\ 0&0&0&0&1&0&0&0&0&0\\ 0&0&0&0&0&1&0&0&0&0\end{bmatrix}\begin{bmatrix}\begin{bmatrix}\dot{x}\\ \dot{y}\\ \dot{z}\\ \dot{\theta}\\ \dot{\phi}\\ \dot{\psi}\\ g\end{bmatrix}\\ \begin{bmatrix}\theta\\ \phi\\ \psi\end{bmatrix}\end{bmatrix} +$$

$$\begin{bmatrix}\frac{\sin\psi\sin\phi+\cos\psi\sin\theta\cos\phi}{m}&0&0&0\\ \frac{\sin\psi\sin\theta\cos\phi-\cos\psi\sin\phi}{m}&0&0&0\\ \frac{\cos\phi\cos\theta}{m}&0&0&0\\ 0&l/I_y&0&0\\ 0&0&l/I_y&0\\ 0&0&0&I_z^{'}\\ 0&0&0&0\\ 0&0&0&0\\ 0&0&0&0\\ 0&0&0&0\end{bmatrix}\begin{bmatrix}u(1)\\ u(2)\\ u(3)\\ u(4)\end{bmatrix}$$

Figure 2 reveals the SIMULINK diagram of Draganflyer III, based on the Equation 2. The four inputs are $u(1)$, $u(2)$, $u(3)$ and $u(4)$ in body-fixed frame and the nine outputs are $u$, $v$, $w$, $x$, $y$, $z$, THETA, PHI and PSI. The definitions of input and output parameters can be found in the Table 1. The model has 12 states. Saturation blocks are inserted before the two outputs (velocity and position in the z position of the earth-fixed frame) to preserve the reality of the actuators.

Equation $\sin\psi\sin\phi + \cos\psi\sin\theta\cos\phi$ and Equation $\sin\psi\sin\theta\cos\phi - \cos\psi\sin\phi$ are implemented in Fcn and Fcn1 blocks in Figure 2 while Fcn2 represents the Equation $\cos\phi\cos\theta$. In Equation 1, the moments of inertia in all axes , the mass and the length from COG of the helicopter to each rotor have to be identified first so that this model reflects the reality of the Draganflyer III. The Matlab M-file 'uavini.m' initializes the above parameters and hence requires running before the SIMULINK model is used. The values of the identification procedure carried on the UAV system are to be recorded in this file.

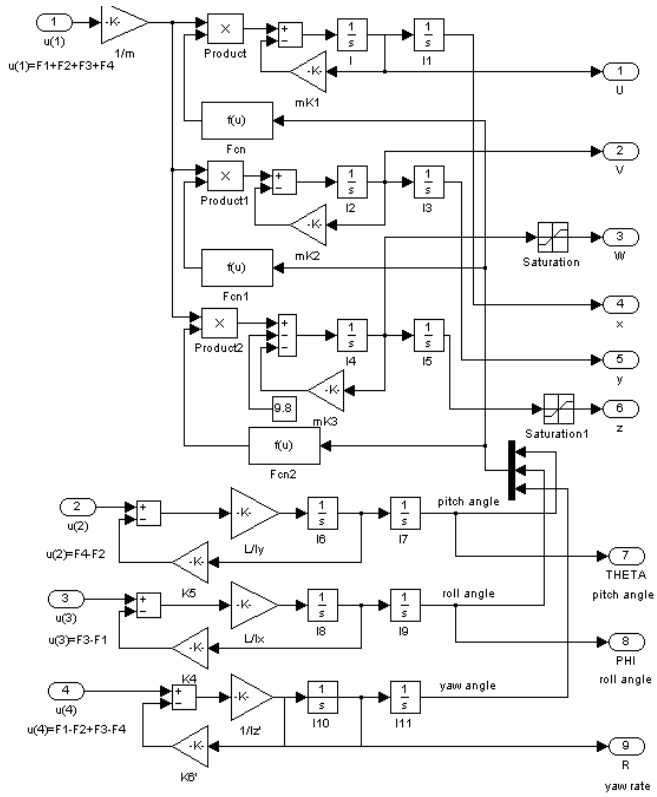


Figure 2: The SIMULINK Model Diagram of The Model

## 3. The Flying Mill

A picture of the flying mill is shown in Figure 3. The steel base and carbon fiber boom limit the flight route of the UAV Draganflyer III to a half sphericity of 1 meter radius.

Two revolute joints at the base and near end of boom provide two degrees of freedom required for flight testing and system identification. In order to mitigate friction in the joints, the revolute joint at the near end of boom uses two low-friction radial ball bearings. The bearings are

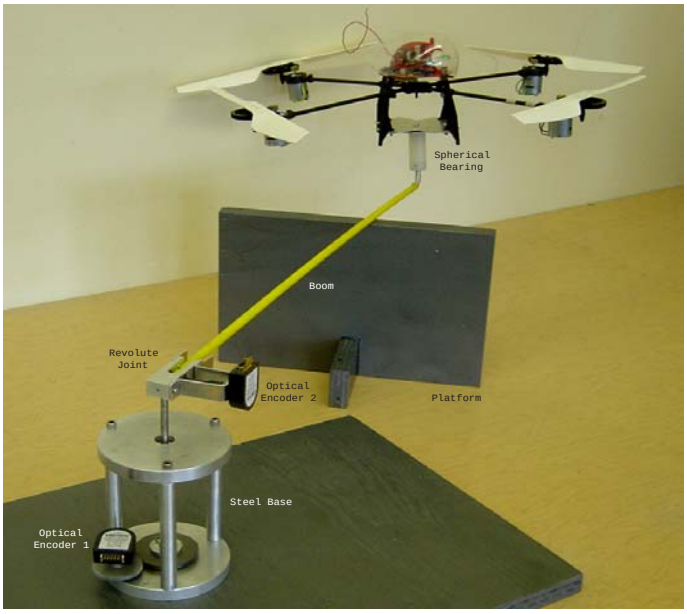


Figure 3: Photo of the flying mill with Draganflyer III

mounted in-line at an appropriate distance apart, parallel to their respective rotational axis, to minimize the moment loads. The far end of the boom is connected to a custom designed spherical bearing which provides the tested UAV enough tilted degrees of freedom and also prevents its four propellers from touching the ground or the boom. Due to the above features of this rig, the modelling and identification performed for the UAV did not justify the modelling of the flying mill. This spherical bearing is made of aluminum to reduce the payload of the tested UAV. The additional payload due to the weight of boom and the spherical bearing is approximately 60 g. The flying mill is mounted on a solid board to prevent overturning during the experiment or a catastrophic failure. Another platform is built to support the UAV during take off and landing. This platform can be replaced by limiting the UAV elevation.

Two optical encoders with resolution of 0.2 degree were used to sense the elevation and angles radial defining the UAV position. One optical encoder is fixed at the bottom of the steel base to record the rotational angle of the vertical shaft. Another optical encoder is mounted at the revolute joint at the near end of the boom to record the vertical position of the tested UAV. The two optical encoders are connected to the D/A dSPACE interface board, DS1102. During the experiment, the position of the UAV is provided by the data from the two optical encoders.The attitude data is updated by three gyroscopes on the UAV. The accelerations along three axes are given by the triaxial accelerometer also placed on the UAV. The encoders were used during the identification and validation of the UAV parameters.

## 4. Two DOF $H_\infty$ Flight Controller For Position Control

The objective of this controller is to achieve a robust control of the four-rotor helicopter, Draganflyer III, at hover even in disturbed air. The loop shown in Figure 4 which is used to control the attitude angles and vertical velocity provides stabilization and decoupling as implemented in [3]. The two degree of freedom architecture is applied for good reference tracking and disturbance rejection. The reference inputs are vertical velocity (W_r), pitch angle (THETA_r), roll angle (PHI_r), yaw rate (R_r) and its control inputs are pedal, longitude, latitude, yaw controls. This controller should fulfil the requirements as follows:

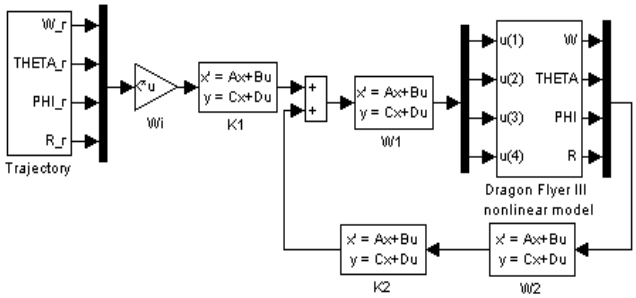


Figure 4: Two DOF $H_\infty$ flight controller loop

- All the closed loop poles must lie in the left half of the s plane to ensure the stability and robustness.
- The closed-up bandwidth shall be as high as practically possible, and hence the rising time in each loop should be around 2 seconds.
- The stability margin $\varepsilon$ is in the interval [0.3, 0.4] allowing for 30-40 % uncertainty in coprime factor.
- Quick pulse and step disturbance rejection.
- The plant was obtained by linearizing the nonlinear model around $u = [4.8000]^T$ equilibrium point. This is equivalent to freezing the scheduling states of the nonlinear controller around these control values.

The design procedure can be described as following:

1. Loop Shaping: The singular values of the unshaped linear model G of Draganflyer III is shown Figure 5. Since the architecture of pitch angle and roll angle loops is identical, the singular values of these two loops overlap each other. Note that during controller parameter tuning, the parameter of these two loops should keep the same. Otherwise, $u(2)$ and $u(3)$ would oscillate heavily around the equilibrium point.

   Using frequency-dependent precompensator $W_1$ and a postcompensator $W_2$, the singular values of the

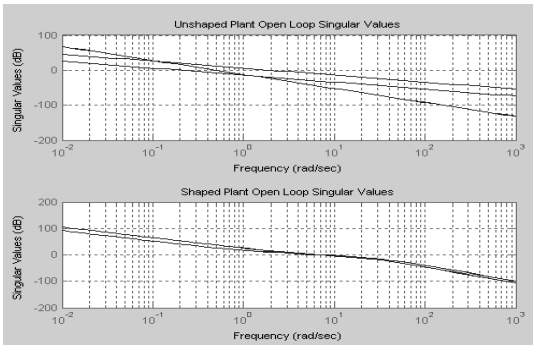


Figure 5: Open Loop Singular Values of the unshaped and shaped plant

shaped plant $G_s$ which is defined as $G_s = W_2 G W_1$ can be shaped to the designed open-loop shape and crossover frequencies at around 7 rad/s in Figure 5. The diagonal precompensator $W_1$ contains proportional and integral (PI) filters. The proportional parts can reduce the phase lag around crossover and set the actuator range. The integral parts can improve the disturbance rejection ability. The post-compensator $W_2$ contains second-order low-pass filters for noise rejection and robustness augmentation and the LHP zeros in pitch angle and roll angle loops to guarantee the slope of -1 in crossover region. The expressions for $W_1$ and $W_2$ are as follows:

$$W_1 = diag\left[\frac{1.5*(1.52s+0.965)}{s} \quad 60 \quad 60 \quad \frac{1.5*(17.2s+9.7)}{s}\right]$$

$$W_2 = diag$$

$$\left[\frac{1000}{s^2+41s+730} \quad \frac{730*(s+2.31)}{s^2+72s+1430} \quad \frac{730*(s+2.31)}{s^2+72s+1430} \quad \frac{1000}{s^2+41s+730}\right]$$

2. Robust Stabilization: Calculate the stability margin $\varepsilon$:

$$\varepsilon^{-1} = \| \begin{pmatrix} I \\ K_\infty \end{pmatrix} (I + P_s K_\infty)^{-1} \widetilde{M}_s^{-1} \|_\infty$$

where $\widetilde{M}_s$ and $\widetilde{N}_s$ is the normalized coprime factors of $P_s$ such that $P_s = \widetilde{M}_s^{-1}\widetilde{N}_s$ and

$$\widetilde{M}_s^{-1}\widetilde{M}_s^* + \widetilde{N}_s^{-1}\widetilde{N}_s^* = I$$

If the stability margin is in the interval [0.3, 0.4], the $H_\infty$ controller $K_\infty$ would guarantee robustness based on theoretical [4] and practical experience [5].

In the case of each open loop, the stability margin $\varepsilon$ has direct relationship with the gain margin (GM) and phase margin (PM) as:

$$GM = \pm 20 \log_{10} \frac{1+\varepsilon}{1-\varepsilon}, \; and \; PM = 2 \arcsin \varepsilon$$

We should note that the calculated GM and PM can also be used to analyze the robustness and stability. Typically we require $GM > 2(6dB)$ and $PM > 45^o$. Opening loop at a time is a common way of testing the closed loop system's margins. The $H_\infty$ optimization gave $\varepsilon = 0.3532$.

3. Implementation: The final feedback controller K is then constructed by combining the $H_\infty$ controller $K_\infty$ with the shaping functions $W_1$ and $W_2$ as:

$$K = W_1 K_\infty W_2$$

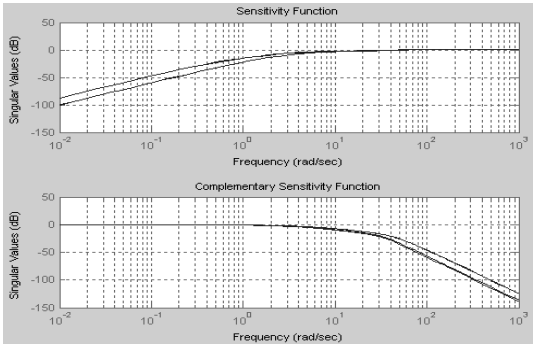


Figure 6: Sensitivity and complementary sensitivity

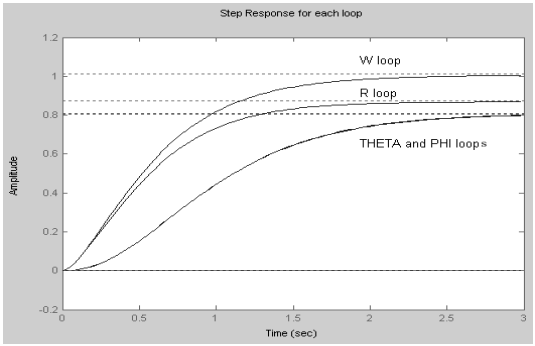


Figure 7: Step responses with $H_\infty$ controller

The resulting closed-loop system was implemented and simulated to verify the robust stability and performance of the achieved controller.

Figure 6 shows the sensitivity and complementary sensitivity for the $H_\infty$ designed controller. The peak of them is close to 1 and thus good disturbance rejection and reference tracking are expected and achieved. Figure 7 compares the step responses of each loop separately with the $H_\infty$ controller in place. The rising time of each step response is around 2 seconds, satisfying the specification. Figure 8 representing the impulse responses of each loop with the controller proves that the controller has quick

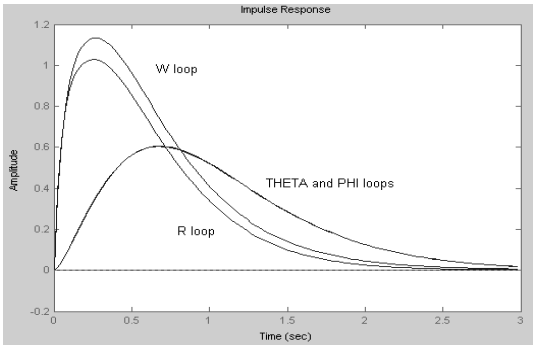


Figure 8: Impulse responses $H_\infty$ controller

pulse disturbance rejection. Figure 9 shows the output step disturbance starting at 12 seconds to each loop. The controller reject the disturbance after 3 seconds. Nonlinear simulations with the nonlinear model were performed using the $H_\infty$ flight controller at hover. Figure 10 shows the simulation results of the four outputs when the reference values of the vertical velocity (W) is fixed to zero and the reference value of the pitch angle ($\theta$) and roll angle ($\phi$) are changed from 0 to 0.5 rad at 15 and 30 seconds respectively. There is also a step from 0 to 0.5 rad/s of the yaw rate at 45 seconds.

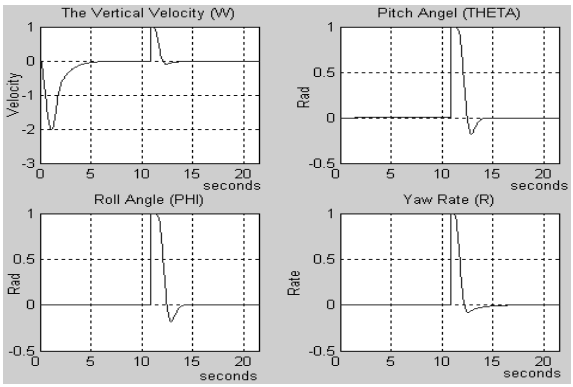


Figure 9: Output step disturbance responses

## 5. Conclusions

A nonlinear modelling of the quad rotor UAV Graganflyer III was presented. A flying mill which is used for flight testing and parameter identification was introduced. Based on this nonlinear model, a $H_\infty$ loop shaping flight controller is achieved for position control. The simulation results prove its robustness, good reference tracking and disturbance rejection.

## References

[1] *Robust Flight Control Design Challenge Problem Formulation and Manual*. Group For Aeronautical Research And Technology In Europe.

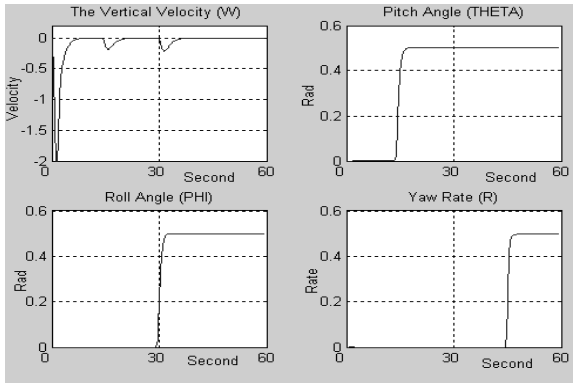


Figure 10: Simulation of nonlinear model

[2] Paul Blue, Levent Güvenc, and Dirk Odenthal. Large envelope flight control satisfying $H_\infty$ robustness and performance specifications. *Proceedings of the American Control Conference, Arlington,VA*, June 25-27,2001.

[3] M. L. Civita, G. Papageorgiou, W. C. Messner, and T. Kanade. Design and flight testing of a gain-scheduled $H_\infty$ loop shaping controller for a robotic helicopter. *Submitted to the 2003 American Control Conference*.

[4] D. McFarlane and K. Glover. A loop shaping design procedure using $H_\infty$ synthesis. *IEEE Trans. on Automatic Control*, 37, June,1992.

[5] G. Papageorgiou and K. Glover. Taking robust LPV control into flight on the VACC Harrier. *Proceedings of the 39th IEEE conference on Decision and Control*, pages 4558–4564, 2000.

[6] UAVs. New world vistas: Air and space for the 21st centry. *Human systems and biotechnology systems*, 7.0:17–18, 1997.

[7] D. Walker and I. Postlethwaite. Advanced helicopter flight control using two-degree-of-freedom $H_\infty$ optimization. *Journal of Guidance, Control and Dyanmics*, 19:461–468, 1996.

[8] Martin F. Weilenmann, Urs Christen, and Hans P. Geering. Robust helicopter postion control at hover. *Proceedings of the American Control Conference, Baltimore,Maryland*, June 1994.